

ZDZISŁAW ADAMCZYK¹, MAGDALENA CEMPA², BARBARA BIAŁECKA³

Synthesis of Na-LSX type zeolite from Polish fly ash

Introduction

The coal combustion process is the basic method of electricity production in Poland. The wastes from this process are slag and exhaust fumes which contain fly ash and gases (N_2 , H_2O , SO_x , NO_x , CO , CO_2 , carbohydrates, and aldehydes). The main disadvantage of the currently used combustion technologies is the emission of pollutants, mainly CO_2 , into the atmosphere, as well as the low efficiency of power units (Kordylewski 2005; Ściążko 2009). In Poland, the wastes resulting from the energetic combustion of coal are mainly neutralized by landfilling and they are therefore seen as a threat to the environment (Łączny 2002). On the other hand, fly ash can be used in environmental protection, including air protection (for desulphurization and removal of CO_2 from exhaust gas), surface waters (for removing the causes of eutrophication of lakes), groundwater (for creating protective barriers) and for the recultivation of degraded areas (Łączny 2002; Lee et al. 2005; Prasad et al. 2012; Łączny et al. 2015; Mishra et al. 2019).

✉ Corresponding Author: Magdalena Cempa; e-mail: mcempa@gig.eu

¹ Central Mining Institute, Katowice, Poland; ORCID iD: 0000-0002-4779-1263; e-mail: mcempa@gig.eu

² Silesian University of Technology, Gliwice, Poland; ORCID iD: 0000-0002-5925-4676;
e-mail: zdzislaw.adamczyk@polsl.pl

³ Central Mining Institute, Katowice, Poland; ORCID iD: 0000-0002-6002-5475; e-mail: bbialecka@gig.eu



© 2020. The Author(s). This is an open-access article distributed under the terms of the Creative Commons Attribution-ShareAlike International License (CC BY-SA 4.0, <http://creativecommons.org/licenses/by-sa/4.0/>), which permits use, distribution, and reproduction in any medium, provided that the Article is properly cited.

The composition of fly ash depends mainly on the type of coal, temperature and the type of atmosphere in the furnace, as well as the flue gas purification technology (SCR or SNCR reactor for NO_x reduction, desulphurization installations, mercury removal, etc.). The final chemical and mineral composition of the ash is formed in the exhaust stream. In the case of fly ash from coal combustion in pulverized-fuel boilers, the content of the crystalline phase is from 15% to 50%. The vitreous phase, which is a residue, is composed mainly of SiO₂ and Al₂O₃ (Łączny 2002).

Zeolites are crystalline, hydrated metal aluminosilicates (mainly groups I and II). These minerals belong to the group of spatial aluminosilicates (skeletal). Their structure consists of tetrahedrons [AlO₄] and [SiO₄], which form rings, and open channels with strictly defined diameters are found between them. The characteristic feature of zeolites associated with their construction is the ability to give away water without changing the shape of the crystal or grain during heating to 400°C and taking it back during cooling. The channels sizes in zeolites range from about 3Å to 10Å. A different degree of silicon and aluminum oxidation gives zeolites an electronegative nature, the size of which is determined by the Al/Si ratio. Therefore, these minerals are characterized by high adsorption capacity and a high ion exchange capacity. In addition, strictly defined channel diameters give the possibility of the selective adsorption of specific ions and molecules (Bolewski and Manecki 1993). Zeolites are used, among others, to remove heavy metals, ammonium ions, radioactive elements, hydrocarbons, organochlorine compounds and the separation of selected gases, among others H₂S, SO₂, CH₄, CO₂, Hg BTEX, as well as an addition to fertilizers, soil cleaning, medicine (Erdem et al. 2004; Franus and Wdowin 2010; Wdowin et al. 2014; De Smedt et al. 2015; Sadeghi et al. 2016; Bandura et al. 2017; Channabasavaraj and Ramalinga 2017; Chen et al. 2017; Collins et al. 2020; Costa et al. 2020; Czuma et al. 2020a, 2020b; Eisenwagen and Pavelić 2020; Ferretti et al. 2020; Kunecki et al. 2020; Pambudi et al. 2020; Vaezihir et al. 2020). Due to their chemical composition (high content of aluminum and silicon), fly ash from coal combustion in pulverized-fuel boilers is a substrate for the synthesis of zeolites and thus finds application in environmental protection. Considering that the main disadvantage of currently used combustion technologies is the emission of large quantities of CO₂ into the atmosphere (for example, in Poland in 2017, the emission was 308.6 mln Mg (BP 2018), the use of zeolites synthesized on the basis of ash for the sorption of this gas is of particular application importance. Among others, zeolites of the faujasite group have appropriate channel sizes to use them for CO₂ sorption (Prats et al. 2017).

The synthetic X-type zeolites belong to the faujasite group (FAU code), the structure of which is as follows: β-cages and hexagonal prisms are connected in such a way that large internal super cages (α-cages) are created. Molecules, including CO₂, can enter the α-cages through 12 Membered Ring (12MR). The windows have a diameter of 7.4Å (Deams et al. 2006). Table 1 presents the chemical formulas of selected synthetic X-type zeolites. These zeolites can basically be divided into two groups: low silicon content (LSX type zeolites) and medium silicon content zeolites (X-type zeolites). The established chemical formulas as well as the chemical composition of X-type zeolites reveal their considerable diversity.

Table 1. Characterization of selected synthetic zeolites, author's own study based on (Yang et al. 2010)

Tabela 1. Charakterystyka wybranych syntetycznych zeolitów

Mineral name	Chemical formula	SiO ₂	Al ₂ O ₃	SiO ₂ + Al ₂ O ₃
		% mass		
Zeolite X	Na ₈₈ (Al ₈₈ Si ₁₀₄ O ₃₈₄)(H ₂ O) _{172,1}	37.72	27.09	64.81
Zeolite X	Ca ₄₀ Al ₈₀ Si ₁₁₂ O ₃₈₄ (H ₂ O) ₁₁₆	44.44	26.94	71.38
Zeolite X	K _{90,1} (Al ₉₂ Si ₁₀₀ O ₃₈₄)	40.21	31.39	71.60
Zeolite Na-LSX	Na ₉₆ (Al ₉₆ Si ₉₆ O ₃₈₄)(H ₂ O) _{384,3}	28.05	23.80	51.85
Zeolite NaK-LSX20	Na ₇₇ K ₁₉ Al ₉₆ Si ₉₆ O ₃₈₄ (H ₂ O) _{396,9}	27.34	23.20	50.54
Zeolite NaK-LSX42	Na ₅₆ K ₄₀ (Al ₉₆ Si ₉₆ O ₃₈₄)(H ₂ O) _{408,7}	26.65	22.61	49.26
Zeolite NaK-LSX80	Na _{24,4} K _{71,6} (Al ₉₆ Si ₉₆ O ₃₈₄)(H ₂ O) _{494,2}	24.34	20.65	44.99
Zeolite NaK-LSX80	Na ₁₉ K ₇₇ (Al ₉₆ Si ₉₆ O ₃₈₄)(H ₂ O) _{385,7}	26.42	22.42	48.85
Zeolite K-LSX	K ₉₆ Al ₉₆ Si ₉₆ O ₃₈₄ (H ₂ O) _{362,3}	26.56	22.54	49.11

The main cations in them can be Na⁺, K⁺ and Ca²⁺, which is important for the content of SiO₂ and Al₂O₃.

The basic method of synthesis of zeolites based on the ash from coal combustion is a hydrothermal conversion (Querol et al. 2001, 2002; Bukhari et al. 2015; Lee et al. 2017; Belviso 2018; Czuma et al. 2020b; He et al. 2020; Lankapati et al. 2020; Miricioiu and Niculescu 2020; Todorova et al. 2020; Verrecchia et al. 2020; Wiśniewska et al. 2020). Kotova et al. (Kotova et al. 2016) studied the effect of synthesis duration (2–12 hours), the concentration of activation solution (1.5–4.5M NaOH) and temperature (80–180°C) on the type of zeolites synthesized on the base of fly ash. The zeolite X was obtained in the temperature range of 90–100°C, and the increase in reaction temperature caused the formation of zeolites with medium (zeolite P – 140°C) and small (analcime and cancrinite – 180°C) channel size. It has also been shown that the type of zeolite and its content in the reaction products are significantly affected by reaction time and alkali concentration. A series of syntheses were carried out at 140°C. Under these conditions, the X zeolite was obtained applying a short reaction time (4 hours) and a high concentration of activating solution (4.5M NaOH). Longer reaction time led to the disappearance of the X zeolite phases and crystallization of the more thermodynamically stable phases (zeolite P followed by analcime).

So far, few syntheses of X-type zeolites from fly ash has been done in Poland (Derkowski et al. 2006, 2007; Franus and Wdowin 2011; Franus 2012; Bukalak et al. 2013; Franus et al. 2014). Zeolithization was carried out on fly ashes from the Kraków CHP plant as well as the Kozienice, Rybnik and Stalowa Wola power plants, in which hard coal is the basic fuel.

The synthesis processes were carried out under various laboratory conditions and a semi-technical scale:

- ◆ amount of fly ash – 10 g, concentration of sodium hydroxide solution – 3M, temperature – 75°C, synthesis duration – 24 h (Derkowski et al. 2006),
- ◆ amount of fly ash – 10 g, ratio of sodium hydroxide with sodium chloride in the ratio of solid to liquid 25–100 g/dm³, temperature 21–22°C, synthesis duration – 2–20 months (Derkowski et al. 2007),
- ◆ amount of fly ash – 10–15 kg, amount of sodium hydroxide – 11 kg, amount of water – 0.9 m³, temperature – 80°C, synthesis duration – 24 h (Franus and Wdowin 2011),
- ◆ amount of fly ash – 20 g, concentration of sodium hydroxide solution – 2–4M or 2–7M, temperature – 50–100°C or 21–22°C, synthesis duration 6–36 h or 1–6 months (Franus 2012),
- ◆ sodium hydroxide was fused with fly ash in a 1.2:1 ratio at 550°C, after grounding the sinter was mixed with water in a ratio of 1:4, synthesis temperature – 90°C, synthesis duration – 24 h,
- ◆ amount of fly ash – 20 g, concentration of sodium hydroxide solution – 3M or 5M, temperature – 75°C or 95°C, synthesis duration – 24 h (Franus et al. 2014).

In the synthesis products, admixtures of sodalite were sometimes found and there were phases that are relics of fly ash (quartz, mullite, amorphous phase, calcite).

The aim of the study was to carry out zeolitization of fly ash using a conventional hydrothermal process in such conditions as to obtain an X-type zeolite in the synthesis products. The process was carried out using various NaOH / fly ash ratios to determine the impact of this ratio on the quality of the synthesis products obtained. For this reason, the identification of phases associated with type X zeolite was important to determine this effect. The test results will also make it possible to assess the repeatability of the conduct under certain process conditions to obtain a product containing X-type zeolite.

1. Sampling and testing methods

A sample of fly ash was taken from one of the Polish coal-fired power plants. The chemical and phase composition of the ash was determined in order to identify the possibility of its zeolitization.

The zeolitization of fly ash (sample IS) was carried out by the hydrothermal method using various NaOH fly ash mass ratio – 3.0 (sample A), 4.0 (sample B) and 6.0 (sample C). The process was carried out under the following permanent conditions temperature: 90°C, time – 16 h, water solution of NaOH (L)/fly ash (g) ratio – 0.025.

The products obtained as a result of zeolitization were the subject of qualitative testing to determine new phases resulting from the process. The tests included observations in a mineralogical microscope, identification of phases by X-ray diffraction, observations and measurements in a scanning electron microscope and thermal analysis.

The microscopic observations of fly ash and products of synthesis were carried out on the Zeiss Axioscope polarizing microscope in the transmitted light. Powder preparations were prepared for this testing.

The identification of phases by X-ray diffraction (XRD) for fly ash and products of synthesis was performed on the Malvern Panalytical Aeris 1 diffractometer with the $\text{Cu}_{K\alpha}$ lamp. The conditions of measurement were as follows: voltage – 40 kV, current – 8 mA, time – 4.84 s, increment of the 2-theta angle – 0.003° , range of 2-theta angle – $4\text{--}74^\circ$. The HighScore Plus software with the database was used to interpret the XRD spectra.

The measurements of mass loss of the tested fly ash and the products of synthesis were made by thermal analysis using the analyzer SDT Q600 by TA Instruments. The conditions of measurement were as follows: mass sample approx. 20 mg, temperature range – $22\text{--}1000^\circ\text{C}$, temperature increase – $10^\circ\text{C}/\text{min}$, atmosphere – air.

Grain morphology and measurements of the chemical composition in the micro-area for the fly ash and the products of synthesis were made using the electron microscope (SEM) SU3500 by Hitachi, equipped with the UltraDry energy dispersive spectrometer (EDS) detector by ThermoFisher Scientific.

2. Results

The chemical composition of the tested fly ash sample, as indicated by multi-year studies (1999–2019), did not show any significant differentiation. The main ash components were SiO_2 and Al_2O_3 , the contents of which were respectively 51.62% by mass and 28.14% by mass (in this study), while so far these contents varied respectively in the range of 49.20–50.70% by mass for SiO_2 and 25.24–26.35% by mass for Al_2O_3 (Table 2). One of the more important chemical components was Fe_2O_3 , the content of which was 6.34% by mass (in this study), and in earlier studies, it ranged from 5.18 to 8.10% by mass. The contents of TiO_2 , MgO , CaO , Na_2O , and K_2O ranged from approx. 1% by mass. to approx. 3% by mass, while the content of other chemical components (MnO , SO_2 , P_2O_5) did not exceed 1% by mass (in this study), and these components were determined at a similar level in the earlier studies (Ratajczak et al. 1999; Wala and Rosiek 2008; Klupa et al. 2017a). The loss on ignition (LOI) in the studied ash was 2.13% by mass and was mainly associated with the unburnt organic matter (carbon), although in the earlier studies it was even 6.80% by mass. The low content of rare earth elements was also found (Klupa et al. 2017b).

The results of chemical composition studies indicate that the $\text{SiO}_2/\text{Al}_2\text{O}_3$ ratio is 1.83 (mol ratio 3.12), which predisposes this fly ash to zeolite conversion (Querol et al. 2002; Bukhari et al. 2015; Belviso 2018; Ren et al. 2020).

Studies on the mineral composition of fly ash also do not indicate a large variation. The microscopic observations in transmitted light revealed that the ash contained mainly mullite and quartz, as well as a significant share of amorphous substance (glass and unburnt organic substance). Mullite and spherical enamel often formed joint aggregates (Fig. 1). In fly ash,

Table 2. Variability of the chemical composition of fly ash in one of the Polish power plants in the years 1999–2018 (% mass)

Tabela 2. Zmienność składu chemicznego popiołu lotnego w jednej z polskich elektrowni w latach 1999–2018 (% masy)

Chemical component	Ratajczak et al. (1999)	Wala and Rosiek (2008)	Klupa et al. (2017a)	Fly ash in this study
SiO ₂	49.60	49.92	50.70	51.62
TiO ₂	1.00	–	0.99	1.21
Al ₂ O ₃	26.35	25.82	25.24	28.14
Fe ₂ O ₃	8.10	5.18	5.68	6.34
MnO	0.10	–	0.06	0.07
MgO	2.68	1.82	2.58	2.37
CaO	4.10	3.92	3.41	3.02
Na ₂ O	2.94	1.10	0.97	1.32
K ₂ O	0.86	3.00	3.71	3.35
SO ₃	–	–	–	0.28
P ₂ O ₅	0.48	–	0.57	0.63
LOI	3.01	6.80	4.79	2.13
Total	99.21	97.56	98.71	100.48
Mol ratio Si/Al	3.20	3.29	3.41	3.12

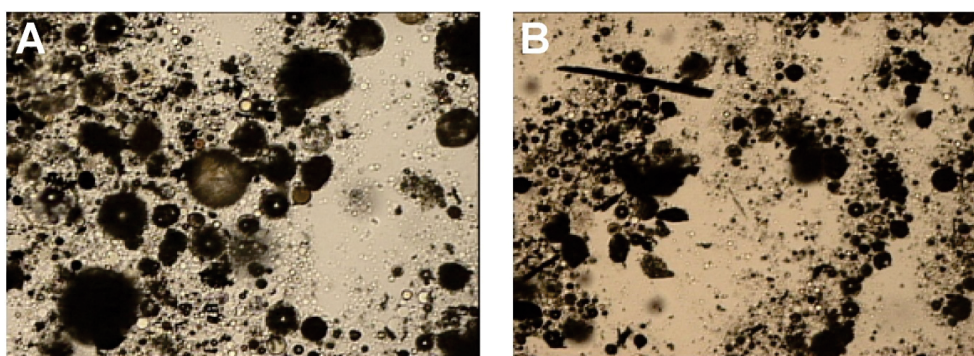


Fig. 1. Microscopic image of the tested fly ash, light passing through one Nicol prism, 200× magnification, (A) in the center a spherical enamel aggregate with mullite, (B) elongated grains of opaque organic matter

Rys. 1. Obraz mikroskopowy badanego popiołu lotnego, światło przechodzące jeden nikol, pow. 200× (A) w centrum kuliste agregaty szkliska z mullitem, (B) wydłużone ziarna nieprzezroczystej substancji organicznej

in addition to quartz and mullite, hematite was also found by the X-ray method. A high background on the diffractogram in the 2-theta angle range of 16–31° proves the presence of an amorphous substance (Fig. 2). Studies by other authors have shown that spinels (magnetite, magnesioferrite, hercynite, pleonaste), wustite, rutile, and florencite may occur in smaller amounts (Ratajczak 1999; Adamczyk and Makosz 2014; Klupa et al. 2017a; Cempa et al. 2018).

The identification of phases by X-ray diffraction revealed the phase composition of the products of synthesis. However, it should be emphasized, that all the synthesized materials contain the mineral components of fly ash (mullite with quartz, as well as magnetite) unreacted in the synthesis. The newly formed mineral components are:

- ◆ in sample A – Na-LSX type zeolite and hielscherite,
- ◆ in sample B – Na-LSX type zeolite, hielscherite and hydrosodalite,
- ◆ in sample C – hydrosodalite (Fig. 2).

This indicates the presence of basic reflections originating from these phases appearing on the diffractograms:

- ◆ Na-LSX type zeolite (Å) – 14.46; 8.86; 7.55; 5.74; 4.43; 3.82; 3.34; 3.06,
- ◆ hielscherite (Å) – 9.62; 5.55; 4.91; 4.60; 3.81; 3.43; 2.74; 2.62; 2.52; 2.17; 2.12,
- ◆ hydrosodalite (Å) – 6.30; 3.63; 2.82; 2.57; 2.10; 1.81; 1.74; 1.57.

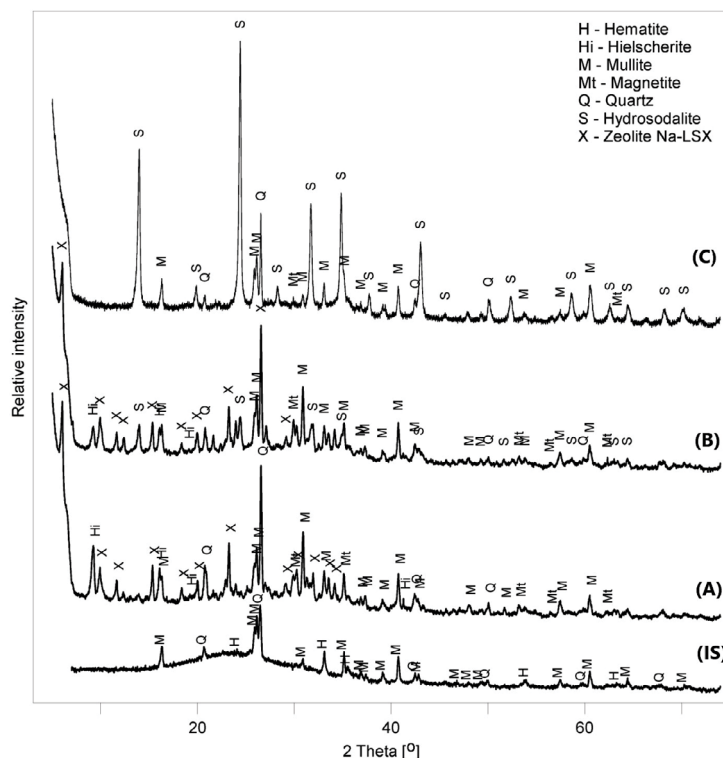


Fig. 2. X-ray diffraction pattern of fly ash (sample IS) and synthesis products (samples: A, B and C)

Rys. 2. Dyfraktometr rentgenowski popiołu lotnego (próbka IS) i produktów syntezy (próbki: A, B i C)

The chemical formulas of the new phases in the products of synthesis are as follows:

- ◆ Na-LSX type zeolite (X) – $\text{Na}_{96}(\text{Al}_{96}\text{Si}_{96}\text{O}_{384}) \cdot 348.3 \text{ H}_2\text{O}$,
- ◆ hielscherite (Hi) – $\text{Ca}_3\text{Si}(\text{OH})_6(\text{SO}_4)(\text{SO}_3) \cdot 11 \text{ H}_2\text{O}$,
- ◆ hydrosodalite (S) – $\text{Na}_6(\text{AlSiO}_4)_6 \cdot 8 \text{ H}_2\text{O}$.

They indicate that the theoretical loss of mass associated with the dehydration of these phases is respectively: X – 33.64% by mass, Hi – 39.38% by mass, and S – 14.46% by mass.

The results of the TGA analysis revealed that the weight loss of fly ash is 1.90%, which corresponds well with the chemical analysis (2.13%). This weight loss was probably mainly associated with the oxidation of unburned coal in ash. The mass stabilizes at a temperature of approx. 700°C.

In the products after synthesis, a much larger mass loss was visible compared to the initial fly ash sample and amounted to a maximum of 17.65% for sample B and a minimum for sample C – 14.62%. The mass losses in these three samples were therefore similar to each other, as was the course of TG curves.

Thermogravimetric studies indicate (Esposito et al. 2004; Bukalak et al. 2013; Fan et al. 2015) that the Na-LSX zeolite has a mass loss of several degrees. The first effect up to about 220°C corresponds mainly to the desorption of physisorbed water, and another one occurred from 220 to 480°C, which was attributed to the dehydration of chemisorbed water. The TG curves of the synthesis products tested have an almost identical course. However, the last effect of mass loss on these curves is noteworthy ending at 700°C, after which the mass stabilizes. It is identical to the ash sample and should be associated with the oxidation of unburned coal in the sample.

The reason for the lower weight loss in sample C was mainly the presence of hydrosodalite synthesis in this product. As indicated by thermogravimetric studies (Majchrzak-Kucęba and Nowak 2004), the weight loss of sodalite is 13.9%, which was similar to the weight loss of this sample.

The share of new phases was calculated in the products after synthesis, taking the mass loss recorded on the TG curves of the tested samples (Fig. 3) and the theoretical dehydration of the new phases into account. These calculations indicate that the share of Na-LSX zeolite in A and B samples is comparable and amounts to 42.9% by mass and 41.0% by mass, respectively (Table 3).

The share of hielscherite in the analyzed samples is also similar and amounts to 6.1% by mass and 5.0% by mass, respectively. However, the share of hydrosodalite varies greatly in the tested samples and a clear increase is seen with the increasing concentration of activating NaOH solution.

Grain morphology of the products after synthesis, revealed in the electron microscope observations, confirms the new phases identified by X-ray diffraction (Khemthong et al. 2007; Musyoka et al. 2011; Pekov et al. 2012; Franus et al. 2014; Kwakye-Awuah et al. 2014; Zgureva and Boycheva 2015; Donkor and Buamah 2016; Salih et al. 2019) in the form of:

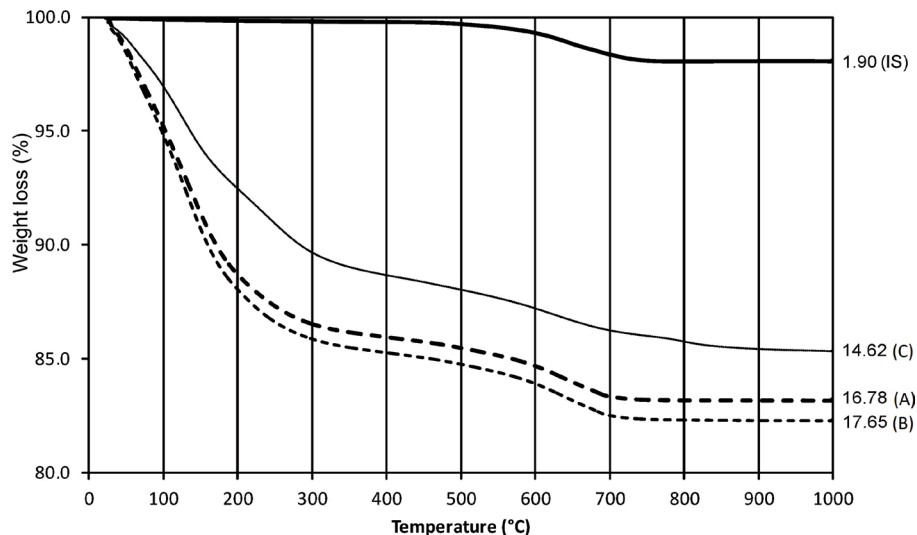


Fig. 3. TGA curves of fly ash (IS) and the products after synthesis (samples: A, B and C)

Rys. 3. Krzywe TGA popiołu lotnego (IS) oraz produktów po syntezie (próbki: A, B i C)

Table 3. Share of new phases in products synthesis calculated on the base of thermal curves, according to samples

Tabela 3. Obliczony na podstawie krzywych termicznych udział nowych faz w produktach syntezy według próbek (% masy)

New phase	Sample		
	A	B	C
Zeolite Na-LSX	42.9	41.0	–
Hielscherite	6.1	5.0	–
Hydrosodalite	–	13.0	54.4
Total	49.0	59.0	54.4

- ◆ cubes – Na-LSX type zeolite (Fig. 4A–C),
- ◆ rods – hielscherite (Fig. 4A and 5C),
- ◆ spherical agglomerates – hydrosodalite (Fig. 4D).

The Na-LSX type zeolite forms crystals with a size of 0.7–4 μm . The smallest ones often form agglomerates, consisting of several or a dozen crystals. The hielscherite rods show a length of 0.4–6 μm , with the sample A being much smaller compared to sample B. The spherical agglomerates of hydrosodalite rarely exceed 3 μm , it is noteworthy that the largest agglomerates occur in sample C. The microscopic observations indicate that the newly formed phases crystallize on the unreacted mineral components of fly ash.

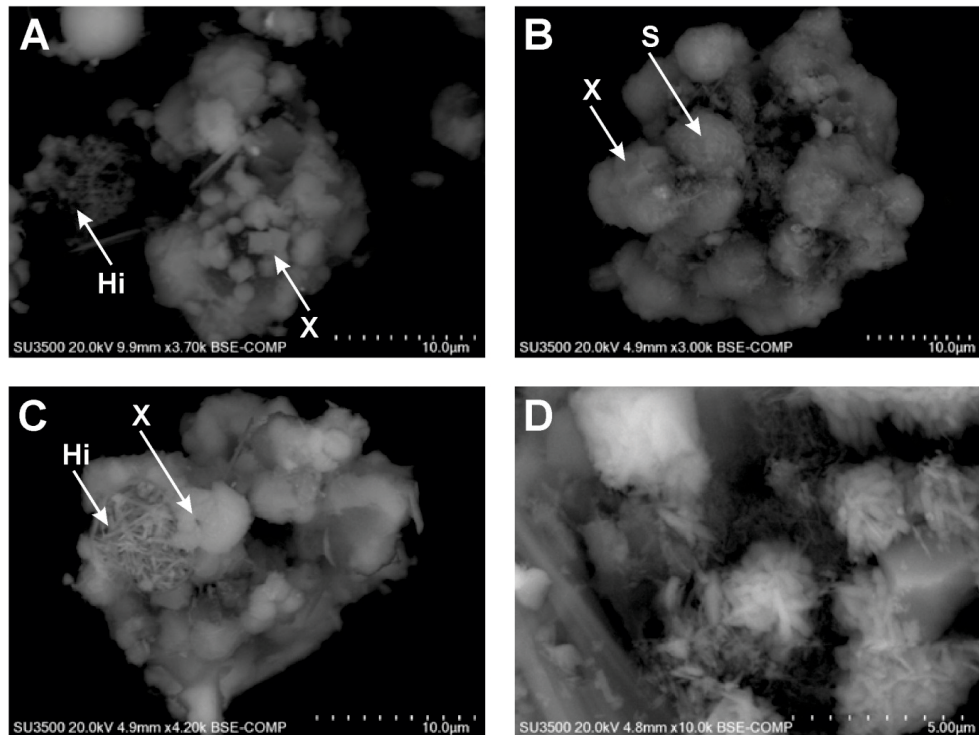


Fig. 4 SEM images of aggregates of the products of synthesis: A) in sample A; B) in sample B; C) in sample B; D) in sample C. Hi – hielscherite, S – hydrosodalite, X – Na-LSX type zeolite.

Rys. 4. Obrazy SEM skupień produktów syntezy: A) w próbce A; B) w próbce B; C) – w próbce B; D) w próbce C. Hi – hielscherite, S – hydrosodalit, X – zeolite typu Na-LSX.

In particular, this is evident in samples A and B, in which common aggregates of mullite, quartz, and enamel are formed with the new phases of tens of micrometers size, and even exceeding 100 μm .

The new phases in products most often create mutual outgrowths. Observations of grain morphology in the electron microscopy reveal a certain order of crystallization of these phases, which is best seen in the sample B in which all three new phases are present. The first to crystallize was hielscherite onto which successively formed the Na-LSX type zeolite, and the whole was covered with hydrosodalite crystallizing at the end.

Mutual outgrowths of the new phases in products are also revealed in the results of tests on the chemical composition in the micro-area (Table 3). These results clearly indicate that the stoichiometric composition of Na-LSX type zeolite, hielscherite or hydrosodalite was not found in any of the tested grains (measuring points). The tested grains are always poly-mineral, and usually one of the new phases dominates in them (Fig. 5). The results of the tests

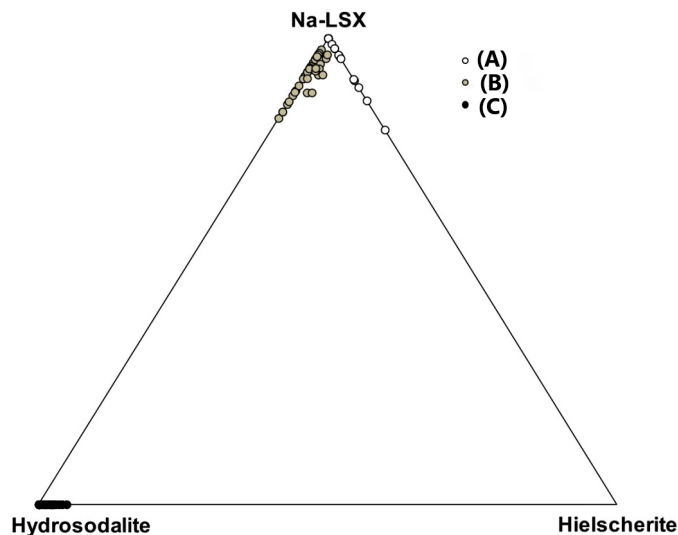


Fig. 5. Projection points of the studied micro-areas in the new phase system of the Na-LSX type zeolite – hydrosodalite – hielscherite according to samples A, B and C

Rys. 5. Punkty projekcyjne badanych mikroobszarów w układzie nowych faz zeolit typu Na-LSX – Hydrosodalit – Hielscherite wg próbek A, B i C

on the chemical composition in micro-areas reveal that apart from hydrosodalite, sample C also contains another newly formed phase – hielscherite.

In each of the tested samples of the synthesis products, two grain populations can be distinguished in terms of chemical composition:

- ◆ containing SO_3 ,
- ◆ not containing SO_3 (Table 4).

However, the main chemical components of the tested grains, irrespective of the samples, are SiO_2 , Al_2O_3 and Na_2O . Their average contents range accordingly 37.51–43.57% by mass, 31.46–37.94% by mass and 9.23–18.10% by mass. The highest SiO_2 content occurs in grains of sample B, Al_2O_3 – in grains of sample A, and Na_2O in – in grains of sample C.

The average contents of other chemical components of the grains do not exceed 7% by mass, and in the case of K_2O and SO_3 rarely exceed 1% by mass. The tendency to decrease the average contents of Fe_2O_3 and K_2O with an increase in the concentration of NaOH of the solution used in the synthesis is noteworthy. Such a variation in the chemical composition of the tested grains may indicate an increase in the share of phases containing sodium with an increase in the concentration of NaOH in the solution, which contributes to an increase in the dissolution of fly ash components containing SiO_2 and Al_2O_3 (mainly enamel and mullite) and overgrowing of the unreacted ash phases with the new phases (Na-LSX type zeolite, hielscherite and hydrosodalite).

The differentiation of SiO_2 , Al_2O_3 and Na_2O contents according to samples A, B and C are presented on the diagrams (Fig. 6A and 6B). The content ranges of these chemical compo-

Table 4. Basic statistical parameters of the chemical composition of the studied micro-areas

Tabela 4. Podstawowe parametry statystyczne składu chemicznego badanych mikroobszarów

Chemical composition	Sample																					
	A						B						C									
	A (without SO ₃)			A (with SO ₃)			B (without SO ₃)			B (with SO ₃)			C (without SO ₃)			C (with SO ₃)						
Min.	Max.	Ave.	Min.	Max.	Ave.	Min.	Max.	Ave.	Min.	Max.	Ave.	Min.	Max.	Ave.	Min.	Max.	Ave.	Min.	Max.	Ave.		
SiO ₂	31.00	47.10	42.18	28.76	44.54	37.51	37.61	49.89	43.57	36.20	47.74	42.47	33.80	44.74	38.93	32.60	44.50	38.14				
TiO ₂	0.50	2.60	1.69	0.90	2.20	1.72	0.37	3.60	1.70	0.42	2.60	1.27	0.42	2.55	1.48	0.67	3.00	1.46				
Al ₂ O ₃	23.20	45.65	31.98	28.28	45.90	37.94	25.10	40.64	31.46	29.68	39.84	34.87	27.44	40.70	33.90	25.40	38.70	33.92				
Fe ₂ O ₃	0.00	12.60	6.72	2.20	8.10	5.86	0.75	10.90	4.96	1.21	7.30	3.61	1.68	5.70	3.78	1.63	6.40	3.50				
MgO	0.80	6.20	3.08	1.01	8.50	3.83	0.13	4.85	1.45	0.42	3.19	1.18	0.55	3.93	1.56	0.35	5.30	2.20				
CaO	0.68	3.54	1.50	0.87	4.49	2.27	0.40	4.10	2.23	0.42	3.91	1.56	0.69	6.60	2.16	0.66	6.14	2.02				
Na ₂ O	5.73	15.37	12.06	5.07	16.31	9.23	10.58	17.80	14.09	12.11	16.44	14.16	14.70	22.22	18.10	14.50	24.30	17.98				
K ₂ O	0.40	1.20	0.80	0.30	1.10	0.61	0.22	0.81	0.51	0.23	0.64	0.39	0.00	0.32	0.09	0.00	0.38	0.12				
SO ₃	–	–	–	0.00	2.34	1.03	–	–	–	0.21	0.78	0.51	–	–	–	0.17	1.52	0.66				
SiO ₂ /Al ₂ O ₃	0.68	1.82	1.39	0.63	1.55	1.03	1.05	1.78	1.40	0.95	1.50	1.23	0.83	1.46	1.16	0.88	1.56	1.14				
	Phase																					
Quartz	6.27	20.13	14.41	3.71	21.46	10.85	6.30	18.40	11.98	3.70	14.29	10.14	0.07	11.07	4.38	0.00	11.02	3.40				
Mullite	5.71	55.42	17.56	12.60	57.00	34.33	1.70	27.37	11.88	7.35	27.73	16.10	0.08	27.03	9.64	0.15	22.30	10.34				
Oxides Fe	6.00	14.80	9.44	6.01	10.30	7.77	0.75	7.90	4.16	1.21	7.30	3.80	1.74	6.33	4.08	1.66	5.77	3.67				
Na-LSX	28.86	69.42	58.10	25.12	65.40	44.38	53.40	81.54	66.33	55.47	75.31	64.86	–	–	–	–	–	–				
Hielscherite	–	–	–	0.82	6.14	2.92	–	–	–	0.52	1.89	1.23	–	–	–	0.44	4.23	1.72				
Hydrosodalite	–	–	–	–	–	–	2.01	12.27	5.64	1.25	6.36	3.86	68.19	95.55	82.72	69.14	94.64	81.06				
Number of analyzes	12			12			31			11			17			18						

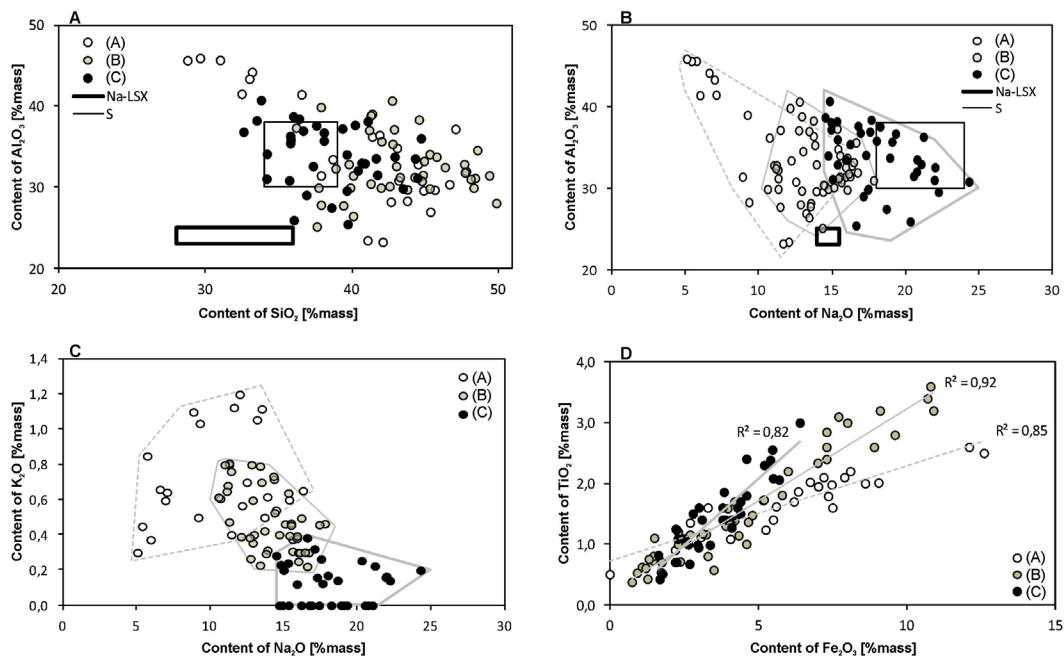


Fig. 6. Differentiation of the contents of chemical components in the studied micro-areas for samples A, B and C: (A) SiO_2 and Al_2O_3 ; (B) Na_2O and Al_2O_3 ; (C) Na_2O and K_2O ; (D) Fe_2O_3 and TiO_2

Rys. 6. Zróżnicowanie zawartości składników chemicznych w badanych mikroobszarach dla próbek A, B i C (A) SiO_2 i Al_2O_3 ; (B) Na_2O i Al_2O_3 ; (C) Na_2O i K_2O ; (D) Fe_2O_3 i TiO_2

nents for zeolite Na-LSX and hydrosodalite are marked schematically on the base of literature data (Vaičiukynienė et al. 2012; Rui et al. 2016; Vaičiukynienė et al. 2016; Yao et al. 2018). Practically none of the tested grains in these systems is in the field corresponding to the Na-LSX type zeolite, while in the hydrosodalite field there are only a dozen grains out of all 101 ones tested (Table 4).

The distribution of potassium contents in the studied grains is interesting in the diagram in the Na_2O – K_2O system according to the samples (Fig. 6C). There is a clear tendency to decrease the K_2O contents in the tested grains while increasing the NaOH concentration in the solutions used for synthesis. The geochemical affinity of these two elements is manifested by mutual substitution in many minerals. Therefore, it can be concluded that in the case of a lower concentration of NaOH in the solution (sample A), potassium probably enters the structure of new phases containing sodium (Na-LSX type zeolite) in larger amounts compared to the new sodium phases formed at a high NaOH concentration in the solution (hydrosodalite).

The substitution of potassium in place of sodium affects the morphology of Na-LSX type zeolite (Basaldella and Tara 1995; Hui et al. 2014). The substitution of Na by K favors, as Basaldella and Tara (Basaldella and Tara 1995) prove, that with the increase in the amount

of K in the LSX type zeolite, the sizes of crystals increase, while their morphology changes from octagons to round shapes. Meanwhile, Hui et al. (Hui et al. 2014) claim that with an increase in the amount of K in place of Na in the LSX type zeolite the octagonal crystals are formed in place of round ones, although at the same time the size of the crystals increases and their walls are smoother. Therefore, it seems that the more important factor determining the morphology of the LSX type zeolite are the conditions of the synthesis. In the first case, the hydrothermal synthesis was carried out at 56°C in various time periods (maximum 196 hours) but it was preceded by calcination of the reagents at 800°C for two hours. In the second case, the reagents were aged at 50°C for 24 hours, followed by the hydrothermal synthesis at 100°C, at various time intervals (maximum 10 hours).

A significant correlation occurs between Fe_2O_3 and TiO_2 ($R^2 > 0.82$), regardless of the concentration of the NaOH solution used for the synthesis (Fig. 6D). As it is known, both of these components are mainly found in Fe oxides (magnetite, hematite) in fly ash. A higher contents of Fe_2O_3 in the A and B samples may indicate that the Fe oxides at such NaOH concentrations of the solution used for synthesis are more stable than the other ash phases. However, the contents of Fe_2O_3 are lower in sample C, which, however, does not necessarily mean the loss of their stability. The crystallization of more new phases (mainly hydrosodalite) is so intense that the share of Fe oxides decreases.

Tests on the chemical composition of the grains in the micro-area revealed that each of them is poly-mineral. The unreacted ash phases (quartz, mullite and Fe oxides) are always found in the grain composition. The average number of these phases in grains decreases with increasing NaOH concentration in the solution. The highest average amounts of quartz, mullite and Fe oxides occurred in the grains of the A sample, their total average amount was between 41% by mass and 53% by mass, with a higher share observed in the grains containing SO_3 compared to the grains without this component (Fig. 7A).

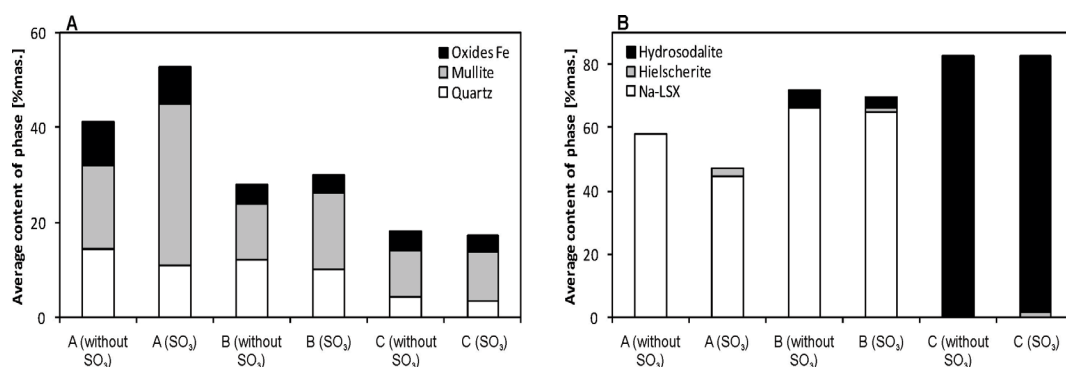


Fig. 7. Average shares of the unreacted fly ash phases (A) and new phases (B) in the products of synthesis by population of sample (samples A, B and C)

Rys. 7. Średnie udziały nieprzereagowanych faz popiołu lotnego (A) i nowych faz (B) w produktach syntezy według populacji próbek A, B i C

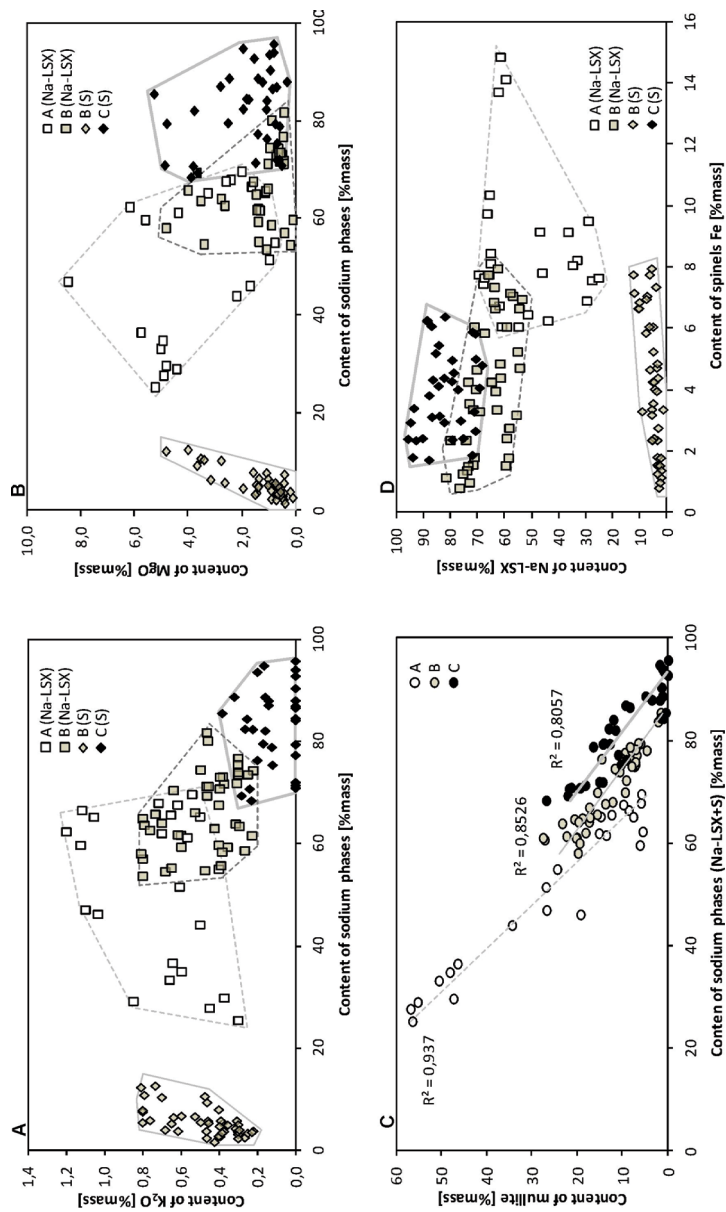


Fig. 8. Differentiation of the contents of the selected chemical components and phases in the studied micro-areas for samples: A, B, C; (A) phases containing sodium and K_2O ; (B) phases containing sodium and MgO ; (C) sum of the phases containing sodium and mullite; (D) Fe spinels and the sum of the phases containing sodium

Rys. 8. Zróżnicowanie zawartości wybranych składników chemicznych i faz w badanych mikroobszarach dla próbek A, B i C (A) fazy zawierające sód i K_2O ; (B) fazy zawierające sód i MgO ; (C) suma faz zawierających sód i mullit; (D) spineli Fe i suma faz zawierających sód

Lower average shares were observed in the grains of sample B (28–30% by mass) and, similarly to sample A, a higher average share was found in the grains containing SO_3 compared to the grains without this component. The lowest average amounts of the unreacted components occurred in the grains of sample C, their total amount was about 18% by mass.

The unreacted fly ash phases are covered with the new ash phases. In the tested grains of samples A and B, the dominant new phase is the Na-LSX type zeolite (Fig. 7B). The average share of this component in the grains of sample B is clearly higher than the average share in sample A. It is noteworthy that in the grains containing SO_3 the share of Na-LSX type zeolite is slightly lower (44.38% by mass for sample A, 64.86% by mass for sample B) than in the grains not containing this component (58.10% by mass for sample A, 66.33% by mass for sample B).

In the grains of sample C, the dominant new phase is hydrosodalite, the average share of which was above 81% by mass. In the case of this sample, as in the case of samples A and B, a slightly less dominant phase are in the grains containing SO_3 .

The composition of the new phases in all samples is supplemented by hielscherite, present in small amounts, containing SO_3 . The average amount of hielscherite tends to decrease phases in synthesis products as the concentration of NaOH in solution increases (Table 4, Fig. 7B).

The new phases containing sodium in the studied grains of the products of synthesis (Na-LSX type zeolite and hydrosodalite) micro-areas show a tendency to decrease the content of potassium and magnesium together with the increase of the share of these phases. The exception is hydrosodalite found in grains of sample B. In this case, with an increase in the share of this component in the grains, both potassium and magnesium tend to increase their quantity (Fig. 8A and 8B).

The decrease in the mullite contents with the increase in the share of the sum of the Na-LSX type zeolite and hydrosodalite is also noteworthy (Fig. 8C). Therefore, it can be assumed that the source of SiO_2 and Al_2O_3 is not only the enamel found in the studied ash but also mullite.

Conclusions

In the studied fly ash, originating from the hard coal combustion, the dominant chemical components were SiO_2 and Al_2O_3 , while the main phase components were mullite, quartz and hematite, and the significant share of an amorphous substance (glass and unburnt organic substance).

In the products after hydrothermal synthesis, the presence of unreacted fly ash phases was found, as well as new phases which quality and quantity depends on the concentration of NaOH in the solution used for synthesis:

- ◆ sample A – Na-LSX type zeolite and hielscherite,
- ◆ sample B – Na-LSX type zeolite, hielscherite and hydrosodalite,
- ◆ sample C – hydrosodalite and hielscherite.

A new aspect at work is the crystallization of hielscherite, which accompanies both Na-LSX zeolite and sodalite. In hydrothermal conversion of fly ash to zeolites, hielscherite has not yet been reported in products.

The grains in all synthesis products are poly-mineral. However, it was found that the new phases, overgrowing the unreacted phase components of fly ash, crystallize in a certain order. Hielscherite is the first crystallizing phase on which the Na-LSX type zeolite crystallizes and the whole is covered with hydrosodalite.

The share of sodium-containing phases (Na-LSX type zeolite and hydrosodalite) in the products of synthesis increases with increasing NaOH concentration in the solution used for the process. A tendency to decrease potassium and magnesium content was observed along with the increase of the share of these phases in grains. The exception is hydrosodalite present in the products formed in sample B because with the increase in the share of this component in grains, both potassium and magnesium contents increase.

It was also found that at a lower concentration of NaOH solution (sample A), sodium can be replaced with potassium in the Na-LSX type zeolite.

The decrease in the mullite content with an increase in the share of the total amount of Na-LSX type zeolite and hydrosodalite may indicate that the source of SiO₂ and Al₂O₃ is not only the glass found in the studied ash but also the mullite.

The results obtained in this study encourage authors to increase the scale of synthesis in order to have more zeolite material available. This material will be used in tests as an addition to concrete to optimize its care and as an admixture to degraded soils for water retention and as a carrier of plant nutrients.

REFERENCES

- Adameczyk, Z. and Makosz, E. 2014. Zeolitization of fly ash using 1M solution of NaOH, [In:] Pozzi, M. ed. *Geochemia i geologia środowiska terenów uprzemysłowionych*. Gliwice: PANOVA, pp. 68–80 (in Polish).
- Bandura et al. 2017 – Bandura, L., Kołodyńska, D. and Franus, W. 2017. Adsorption of BTX from aqueous solutions by Na-P1 zeolite obtained from fly ash. *Process Safety and Environmental Protection* 109, pp. 214–223.
- Basaldella, E.I. and Tara, J.C. 1995. Synthesis of LSX zeolite in the Na/K system: Influence of the Na/K ratio. *Zeolites* 15, pp. 243–246.
- Belviso, C. 2018. State-of-the-art applications of fly ash from coal and biomass: A focus on zeolite synthesis processes and issues. *Progress in Energy and Combustion Science* 65, pp. 109–135.
- Bolewski, A. and Manecki, A. 1993. Detailed mineralogy (*Minerologia szczegółowa*). Warszawa: PAE (in Polish).
- BP 2018 – BP. Statistical Review of World Energy, 2018. London.
- Bukalak et al. 2013 – Bukalak, D., Majchrzak-Kuceba, I. and Nowak, W. 2013. Assessment of the sorption capacity and regeneration of carbon dioxide sorbents using thermogravimetric methods. *Journal of Thermal Analysis and Calorimetry* 113, pp. 157–160.
- Bukhari et al. 2015 – Bukhari, S.S., Behin, J., Kazemian, H. and Rohani, S. 2015. Conversion of coal fly ash to zeolite utilizing microwave and ultrasound energies: A review. *Fuel* 140, pp. 250–266.
- Cempa et al. 2018 – Cempa, M., Adameczyk, Z. and Białecka, B. 2018. Florencite in fly ash from the Rybnik Power plant (Poland). [In:] *Science and Technologies in Geology, Exploration and Mining* 18(1.4). Albena, 2–8 July, 2018. Bulgaria: 18th International Multidisciplinary Scientific Geoconference SGEM, pp. 75–82.

- Channabasavaraj, W. and Ramalinga, R. 2017. A review on characterization and application of fly ash zeolites. *International Journal of Development Research* 7(8), pp.14294–14300.
- Chen et al. 2017 – Chen, H., Wang, W., Ding, J., Wei, X. and Lu, J. 2017. CO₂ Adsorption Capacity of FAU Zeolites in Presence of H₂O: A Monte Carlo Simulation Study. *Energy Procedia* 105, pp. 4370–4376.
- Collins et al. 2020 – Collins, F., Rozhkovskaya, A., Outram, J.G. and Millar, G.J. 2020. A critical review of waste resources, synthesis, and applications for Zeolite LTA. *Microporous and Mesoporous Materials* 291, 109667.
- Costa et al. 2020 – Costa, J.A.S., de Jesus, R.A., Santos, D.O., Mano, J.F., Romão, L.P.C. and Paranhos, C.M. 2020. Recent progresses in the adsorption of organic, inorganic, and gas compounds by MCM-41-based mesoporous materials. *Microporous and Mesoporous Materials* 291, 109698.
- Czuma et al. 2020a – Czuma, N., Casanova, I., Baran, P., Szczurowski, J. and Zarębska, K. 2020a. CO₂ sorption and regeneration properties of fly ash zeolites synthesized with the use of differentiated methods. *Scientific Reports* 10, 1825.
- Czuma et al. 2020b – Czuma, N., Franus, W., Baran, P., Ćwik, A. and Zarębska, K. 2020b. SO₂ sorption properties of fly ash zeolites. *Turkish Journal of Chemistry* 44, pp. 155–167.
- Daems et al. 2006 – Daems, I., Leflaive, P., Methivier, A., Baron, G. V. and Denayer, J.F.M. 2006. Influence of Si:Al-ratio of faujasites on the adsorption of alkanes, alkenes and aromatics. *Microporous and Mesoporous Materials* 96, pp. 149–156.
- Derkowski et al. 2006 – Derkowski, A., Franus, W., Beran, E. and Czimerová, A. 2006. Properties and potential applications of zeolitic materials produced from fly ash using simple method of synthesis. *Powder Technol.* 166, pp. 47–54.
- Derkowski et al. 2007 – Derkowski, A., Franus, W., Waniak-Nowicka, H. and Czimerová, A. 2007. Textural properties vs. CEC and EGME retention of Na-X zeolite prepared from fly ash at room temperature. *Int. J. Miner. Process.* 82(2), pp. 57–68.
- De Smedt et al. 2005 – De Smedt, C., Ferrer, F., Leus, K. and Spanoghe, P. 2005. Removal of Pesticides from Aqueous Solutions by Adsorption on Zeolites as Solid Adsorbents. *Adsorption Science and Technology* 33(5), pp. 457–485.
- Donkor, E.A. and Buamah, R. 2016. Defluorination of drinking water using surfactant modified zeolites. *Journal of Science and Technology* 36(1), pp. 15–21.
- Eisenwagen, S. and Pavelić, K. 2020. Potential Role of Zeolites in Rehabilitation of Cancer Patients. *Arch Physiother Rehabil* 3(2), pp. 29–40.
- Erdem et al. 2004 – Erdem, E., Karapinar, N. and Donat, R. 2004. The removal of heavy metal cations by natural zeolites, *Journal of Colloid and Interface Science* 280(2), pp. 309–314.
- Espósito et al. 2004 – Espósito, S., Ferone, C., Pansini, M., Bonaccorsi, L. and Proverbio, E. 2004. A comparative study of the thermal transformations of Ba-exchanged zeolites A, X and LSX. *Journal of the European Ceramic Society* 24(9), pp. 2689–2697.
- Fan et al. 2015 – Fan, M., Sun, J., Bai, S. and Panzai, H. 2015. Size effects of extraframework monovalent cations on the thermal stability and nitrogen adsorption of LSX zeolite. *Microporous and Mesoporous Materials* pp. 44–49.
- Ferretti et al. 2020 – Ferretti, G., Galamini, G., Medoro, V., Coltorti, M., Di Giuseppe, D. and Faccini, B. 2020. Impact of Sequential Treatments with Natural and Na-Exchanged Chabazite Zeolite-Rich Tuff on Pig-Slurry Chemical Composition. *Water* 12, 310.
- Franus, W. 2012. Characterization of X-type Zeolite Prepared from Coal Fly Ash. *Polish Journal of Environmental Studies* 21(2), pp. 337–343.
- Franus et al. 2014 – Franus, W., Wdowin, M. and Franus, M. 2014. Synthesis and characterization of zeolites prepared from industrial fly ash. *Environmental Monitoring and Assessment* 186, pp. 5721–5729.
- Franus, W. and Wdowin, M. 2010. Removal of ammonium ions by selected natural and synthetic zeolites. *Gospodarka Surowcami Mineralnymi – Mineral Resources Management* 26(4), pp. 133–148.
- Franus, W. and Wdowin, M. 2011. Application of F class fly ash to production of zeolitic material at semi-technical scale (*Wykorzystanie popiołów lotnych klasy F do produkcji materiału zeolitowego na skalę półtechniczną*). *Polityka Energetyczna – Energy Policy Journal* 14(2), pp. 79–91 (in Polish).
- He et al. 2020 – He, X., Yao, B., Xia, Y., Huang, H., Gan, Y. and Zhang, W. 2020. Coal fly ash derived zeolite for highly efficient removal of Ni²⁺ in waste water. *Powder Technology* 367, pp. 40–46.

- Hui et al. 2014 – Hui, H., Gao, J., Wang, G., Liua P. and Zhang, K. 2014. Effects of Na and K ions on the Crystallization of Low-silica X Zeolite and its Catalytic Performance for Alkylation of Toluene with Methanol. *Journal of the Brazilian Chemical Society* 25(1), pp. 65–74.
- Khemthong et al. 2007 – Khemthong, P. Prayoonpokarach, S. and Wittayakun, J. 2007. Synthesis and characterization of zeolite LSX from rice husk silica. *Suranaree Journal of Science and Technology* 14(4), pp. 367–379.
- Klupa et.al 2017a – Klupa, A., Adamczyk, Z. and Harat, A. 2017a. Spinels in the fly ash of Power Plant Rybnik (Poland). [In:] *Science and Technologies in Geology, Exploration and Mining 17(11)*. Albena, 27.06–06.07, 2017. Bulgaria: 17th International Multidisciplinary Scientific Geoconference SGEM, pp. 1051–1058.
- Klupa et.al 2017b – Klupa, A., Adamczyk, Z. and Harat, A. 2017b. Lanthanides in mineral elements found in fly ashes from the Rybnik Power Plant. [In:] *Science and Technologies in Geology, Exploration and Mining 17(11)*. Albena, 27.06–06.07, 2017. Bulgaria: 17th International Multidisciplinary Scientific Geoconference SGEM, pp. 883–888.
- Kordylewski, W. 2005. Burning and fuel (*Spalanie i paliwa*). Wrocław: Oficyna Wydawnicza Politechniki Wrocławskiej, 457 pp. (in Polish).
- Kotova et al. 2016 – Kotova, O.B., Shabalin, I.N., Shushkov, D.A. and Kocheva, L.S. 2016. Hydrothermal synthesis of zeolites from coal fly ash. *Advances in Applied Ceramics* 115(3), pp. 152–157.
- Kunecki et al. 2020 – Kunecki, P., Czarna-Juszkiewicz, D. and Wdowin, M. 2020. Analysis of solid sorbents for control and removal processes for elemental mercury from gas streams: a review. *International Journal of Coal Science & Technology* 922.
- Kwakye-Awuah et al. 2014 – Kwakye-Awuah, B., Labik, L., Nkrumah, I. and Williams, C. 2014. Removal of Arsenic in river water samples obtained from a mining community in Ghana 188 using laboratory synthesized zeolites. *International Journal of Advanced Scientific and Technical Research* 4(4), pp. 304–315.
- Lankapati et al. 2020 – Lankapati, H.M., Lathiya, D.R., Choudhary, L., Dalai, A.K. and Maheria, K.C. 2020. Moronite-Type Zeolite from Waste Coal Fly Ash: Synthesis, Characterization and Its Application as a Sorbent in Metal Ions Removal. *Chemistry Select* 5(3), pp. 1193–1198.
- Lee et al. 2017 – Lee, Y.-R., Soe, J.T., Zhang, S., Ahn, J.-W., Park, M.B. and Ahn, W.-S. 2017. Synthesis of nanoporous materials via recycling coal fly ash and other solid wastes: A mini review. *Chemical Engineering Journal* 317, pp. 821–843.
- Lee et al. 2005 – Lee, K.T., Rahman, A., Bhatia, M.S. and Chu, K.H. 2005. Removal of sulfur dioxide by fly ash/CaO/CaSO₄ sorbents. *Chemical Engineering Journal* 114(1), pp. 171–177.
- Łączny et al. 2015 – Łączny, J.M., Iwaszenko, S., Gogola, K., Bajerski, A., Janoszek, T., Klupa, A. and Cempa-Balewicz, M. 2015. Study on the possibilities of treatment of combustion by-products from fluidized bed boilers into a product devoid of free calcium oxide. *Journal of Sustainable Mining* 14(4), pp. 164–172.
- Łączny, M.J. 2002. Unconventional methods of using fly ash (*Niekonwencjonalne metody wykorzystywania popiołów lotnych*). Katowice: GIG (in Polish).
- Majchrzak-Kućęba, I. and Nowak, W. 2004. Application of model-free kinetics to the study of dehydration of fly ash-based zeolite. *Thermochimica Acta* 413(1–2), pp. 23–29.
- Miricioiu, M.G. and Niculescu, V.C. 2020. Fly Ash, from Recycling to Potential Raw Material for Mesoporous Silica Synthesis. *Nanomaterials* 10(3), 474.
- Mishra et al. 2019 – Mishra, V.K., Jha, S.K., Damodaran, T., Singh, Y.P., Srivastava, S., Sharma, D.K. and Prasad, J. 2019. Feasibility of coal combustion fly ash alone and in combination with gypsum and green manure for reclamation of degraded sodic soils of the Indo-Gangetic Plains: A mechanism evaluation. *Land Degradation & Development* 30(11), pp. 1300–1312.
- Musyoka et al. 2011 – Musyoka, N.M., Petrik, L.F., Balfour, G., Gitari, W.M. and Hums, E. 2011. Synthesis of hydroxy sodalite from coal fly ash using waste industrial brine solution. *Journal of Environmental Science and Health, Part A* 46(14), pp. 1699–1707.
- Pambudi et al. 2020 – Pambudi, T., Wahyuni, E.T. and Mudasir, M. 2020. Recoverable Adsorbent of Natural Zeolite/Fe₃O₄ for Removal of Pb(II) in Water. *Journal of Materials and Environmental Sciences* 11(1), pp. 69–78.
- Pekov et al. 2012 – Pekov, I.V., Chukanov, N.V., Britvin, S.N., Kabalov, Y., Göttlicher, J., Yapaskurt, V., Zadov, A.E., Krivovichev, S., Schüller, W. and Ternes, B. 2012. The sulfite anion in ettringite-group minerals: a new mine-

- ral species hielscherite $\text{Ca}_3\text{Si}(\text{OH})_6(\text{SO}_4)(\text{SO}_3)\cdot 11\text{H}_2\text{O}$, and the thaumasite-hielscherite solid-solution series. *Mineralogical Magazine* 76, pp. 1133–1152.
- Prasad et al. 2012 – Prasad, B., Sangeeta, K. and Tewary, B.K. 2012. Fly Ash Zeolite as Permeable Reactive Barrier for Prevention of Groundwater Contamination Due to Coal Ash Disposal. *Asian Journal of Chemistry* 24(3), pp. 1045–1050.
- Prats et al. 2017 – Prats, H., Bahamon, D., Alonso, G., Giménez, X., Gamallo, P. and Sayós, R. 2017. Optimal Faujasite structures for post combustion CO_2 capture and separation in different swing adsorption processes. *Journal of CO_2 Utilization* 19, pp. 100–111.
- Querol et al. 2001 – Querol, X., Umana, J.C., Plana, F., Alastuey, A., Lopez-Soler, A., Medinaceli, A., Valero, A., Domingo, M.J. and Garcia-Rojo, E. 2001. Synthesis of zeolites from fly ash at pilot plant scale. Examples of potential applications. *Fuel* 80(6), pp. 857–865.
- Querol et al. 2002 – Querol, X., Moreno, N., Umana, J.C., Alastuey, A., Hernandez, E., Lopez-Soler, A. and Plana, F. 2002. Synthesis of zeolites from coal fly ash: an overview. *International Journal of Coal Geology* 50, pp. 413–423.
- Ratajczak et al. 1999 – Ratajczak, T., Gaweł, A., Górnjak, K., Muszyński, M., Szydłak, T. and Wyszomirski, P. 1999. Fly ashes and beidellite clays from Bełchatów as components of self-solidification mixtures (*Charakterystyka popiołów lotnych ze spalania niektórych węgla kamiennych i brunatnych*). *Polskie Towarzystwo Mineralogiczne – Prace Specjalne* 13, pp. 9–34 (in Polish).
- Ren et al. 2020 – Ren, X., Qu, R., Liu, S., Zhao, H., Wu, W., Song, H., Zheng, C., Wu, X. and Gao, X. 2020. Synthesis of Zeolites from Coal Fly Ash for the Removal of Harmful Gaseous Pollutants: A Review. *Aerosol and Air Quality Research* 20, pp. 1127–1144.
- Rui et al. 2016 – Rui, M., Zhu, J., Wu, B. and Li, X. 2016. Adsorptive Removal of Organic Chloride from Model Jet Fuel by Na-LSX Zeolite: Kinetic, Equilibrium and Thermodynamic Studies. *Chemical Engineering Research & Design: Transactions of the Institution of Chemical Engineers Part A* 114, pp. 321–330.
- Salih et al. 2019 – Salih, A.O., Williams, C.D. and Khanaqa, P.A. 2019. Synthesis of Zeolite Na-LSX from Iraqi Natural Kaolin using Alkaline Fusion Prior to Hydrothermal Synthesis Technique. *UKH Journal of Science and Engineering* 3(1), pp. 10–17.
- Sadeghi et al. 2016 – Sadeghi, M., Yekta, S., Ghaedi, H. and Babanezhad, E. 2016. Effective removal of radioactive ^{90}Sr by CuO NPs/Ag-clinoptilolite zeolite composite adsorbent from water sample: isotherm, kinetic and thermodynamic reactions study. *International Journal of Industrial Chemistry* 7, pp. 315–331.
- Ściążko, M. 2009. Technological and economic barriers capture in energy systems (*Technologiczne i ekonomiczne bariery usuwania diutlenku węgla w układach energetycznych*). *Polityka Energetyczna – Energy Policy Journal* 12(2/1), pp. 73–89 (in Polish).
- Todorova et al. 2020 – Todorova, S., Barbov, B., Todorova, T., Kolev, H., Ivanova, I., Shopska, M. and Kalvachev, Y. 2020. CO oxidation over Pt-modified fly ash zeolite X. *Reaction Kinetics, Mechanisms and Catalysis* 129(1), pp. 773–786.
- Wala, D. and Rosiek, G. 2008. Adhesion of the geopolymer composites to concrete, steel and ceramics (*Adhezja kompozytów geopolimerowych do betonu, stali i ceramiki*). *Kompozyty* 8(1), pp. 36–40 (in Polish).
- Wdowin et al. 2014 – Wdowin, M., Wiatros-Motyka, M.M., Panek, R., Tevens, L., Franus, W. and Snape, C.E. 2014. Experimental study of mercury removal from exhaust gases. *Fuel* 128, pp. 451–457.
- Wiśniewska et al. 2020 – Wiśniewska, M., Urban, T., Chibowski, S., Fijałkowska, G., Medykowska, M., Nosal-Wiercinska, A., Franus, W., Panek, R. and Szewczuk-Karpisz, K. 2020. Investigation of adsorption mechanism of phosphate(V) ions on the nanostructured Na-A zeolite surface modified with ionic polyacrylamide with regard to their removal from aqueous solution. *Applied Nanoscience* DOI: 10.1007/s13204-020-01397-9.
- Vaezihir et al. 2020 – Vaezihir, A., Bayanlou, M.B., Ahmadnezhad, Z. and Barzegari, G. 2020. Remediation of BTEX plume in a continuous flow model using zeolite-PRB. *Journal of contaminant hydrology* 230, DOI: 10.1016/j.jconhyd.2020.103604.
- Vaičiukynienė et al. 2012 – Vaičiukynienė, D., Skipkiūnas, G., Sasnauskas, V. and Daukšys, M. 2012. Cement compositions with modified hydrosodalite. *Chemija* 23(3), pp. 147–154.
- Vaičiukynienė et al. 2016 – Vaičiukynienė, G., Vaitkevičius, V., Rudžionis, Ž., Vaičiukynas, V., Navickas, A. and Nizevičienė, D. 2016. Blended Cement Systems with Zeolitized Silica Fume. *Materials Science (Medžiagotyra)* 22(2), pp. 299–304.

- Verrecchia et al. 2020 – Verrecchia, G., Cafiero, L., Caprariis, B., Dell’Era, A., Pettiti, I., Tuffi, R. and Scarsella, M. 2020. Study of the parameters of zeolites synthesis from coal fly ash in order to optimize their CO₂ adsorption. *Fuel* 276, DOI: 10.1016/j.fuel.2020.118041.
- Yao et al. 2018 – Yao, G., Lei, J., Zhang, X., Sun, Z. and Zheng, S. 2018. One-step hydrothermal synthesis of zeolite X powder from natural low-grade diatomite. *Materials* 11, pp. 906.
- Yang et al. 2010 – Yang, S., Vaisman, I., Blaisten-Barojas, E., Li, X. and Karen, V.L. 2010. Framework-Type Determination for Zeolite Structures in the Inorganic Crystal Structure Database. *Journal of Physical and Chemical Reference Data* 39(3), pp. 1–45.
- Zgureva, D. and Boycheva, S. 2015. Synthetic zeolitic ion-exchangers from coal ash for decontamination of nuclear wastewaters. *BgNS Transactions* 20(2), pp. 132–136.

SYNTHESIS OF NA-LSX TYPE ZEOLITE FROM POLISH FLY ASH

Keywords

fly ash, zeolite Na-LSX, hydrosodalite, hielscherite

Abstract

The paper presents the results of hydrothermal zeolitization of fly ash from hard coal combustion in one of the Polish power plants. The synthesis was carried out using various NaOH fly ash mass ratio (3.0, 4.0 and 6.0) and the effect of NaOH concentration in the activating solution on composition of synthesized sample was tested. The process was carried out under the following permanent conditions temperature: 90°C, time – 16 hours, water solution of NaOH (L)/fly ash (g) ratio – 0.025. In the studied fly ash the dominant chemical components were SiO₂ and Al₂O₃, while the main phase components were mullite, quartz and hematite, and a significant share of amorphous substance (glass and unburnt organic substance). After hydrothermal synthesis, the presence of unreacted fly ash phases was found in the products, as well as new phases, the quality and quantity of which depend on the NaOH to fly ash mass ratio used for synthesis:

- ◆ for ratio 3.0 – Na-LSX type zeolite and hielscherite,
- ◆ for ratio 4.0 – Na-LSX type zeolite, hielscherite and hydrosodalite,
- ◆ for ratio 6.0 – hydrosodalite and hielscherite.

The grains in all products of synthesis are poly-mineral. However, it was found that the new phases, overgrowing the unreacted phase components of fly ash, crystallize in a certain order. Hielscherite is the first crystallizing phase, on which the Na-LSX type zeolite crystallizes then, and the whole is covered by hydrosodalite. In the products of synthesis, the share of sodium-containing phases (the Na-LSX type zeolite and hydrosodalite) increases with the increasing concentration of NaOH in the solution used for the process.

SYNTEZA ZEOLITU NA-LSX NA BAZIE POLSKIEGO POPIOŁU LOTNEGO

Słowa kluczowe

popiół lotny, Na-LSX zeolit, hydrosodalit, hielscherit

Streszczenie

W pracy przedstawiono wyniki badań hydrotermalnej zeolityzacji popiołu lotnego pochodzącego ze spalania węgla kamiennego w jednej z polskich elektrowni. Syntezę przeprowadzono przy różnych stosunkach wagowych NaOH/popiół lotny (3,0, 4,0 i 6,0) i badano wpływ stężenia NaOH w roztworze aktywującym na skład zsyntetyzowanej próbki. Proces był prowadzony w następujących warunkach: temperatura syntezy – 90°C, czas syntezy – 16 godzin, stosunek roztworu NaOH (L)/popiół lotny (g) – 0,025. W badanym popiole lotnym dominującymi składnikami chemicznymi były SiO₂ i Al₂O₃, natomiast głównymi składnikami fazowymi były mullit, kwarc, hematyt oraz stwierdzono znaczny udział substancji amorficznej (szkliwi i nieprzepełona substancja organiczna). W produktach po hydrotermalnej syntezie stwierdzono obecność nieprzereagowanych faz popiołu lotnego, a także nowe fazy, których jakość i ilość uzależnione są od stosunku masowego NaOH do popiołu lotnego:

- ♦ dla stosunku 3.0 – zeolit typu Na-LSX i hielscherite,
- ♦ dla stosunku 4.0 – zeolit typu Na-LSX, hielscherite i hydrosodalit,
- ♦ dla stosunku 6.0 – hydrosodalit i hielscherite.

Ziarna we wszystkich produktach syntezy są polimineralne. Stwierdzono jednak, że nowe fazy, obrastające nieprzereagowane składniki fazowe popiołu lotnego, krystalizują w określonej kolejności. Hielscherite jest pierwszą krystalizującą fazą, na którym krystalizuje zeolit typu Na-LSX i całość oblepia hydrosodalit. W produktach syntezy udział faz zawierających sól (zeolit typu Na-LSX i hydrosodalit) wzrasta wraz ze wzrostem stężenia NaOH w roztworze użytym w procesie.